Journal of Applied Electrochemistry **33**: 505–514, 2003.

Effects of a fuel cell test on the structure of irradiation grafted ion exchange membranes based on different fluoropolymers

T. KALLIO[1,*], K. JOKELA[2], H. ERICSON[3], R. SERIMAA[2], G. SUNDHOLM[1], P. JACOBSSON[3] and F. SUNDHOLM[4]

[1]*Laboratory of Physical Chemistry and Electrochemistry, Helsinki University of Technology, PB 6100, FIN-02015 HUT, Finland*

[2]*Division of X-ray Physics, Department of Physical Sciences, University of Helsinki, PB 64, FIN-00014 HU, Finland*

[3]*Department of Experimental Physics, Chalmers University of Technology, SE-412 96 Göteborg, Sweden*

[4]*Laboratory of Polymer Chemistry, University of Helsinki, PB 55, FIN-00014 HU, Finland*

*(*author for correspondence, e-mail: Tanja.Kalli@hut.fi)*

Received 10 July 2002; accepted in revised form 29 December 2002

Key words: fluoropolymers, fuel cell, ion-exchange membrane

Abstract

The role of the fluoropolymer matrix in the stability of irradiation grafted proton conducting membranes under fuel cell conditions is investigated. The structure of a series of membranes with poly(vinylidene fluoride), poly(vinylidene fluoride-co-hexafluoropropylene), poly(tetrafluoroethylene-co-hexafluoropropylene), and poly(ethylene-alt-tetrafluoroethylene) matrices with poly(styrene sulfonic acid) side chains is studied before and after a fuel cell test using X-ray scattering techniques and confocal micro-Raman spectroscopy. All tested membranes suffer from a loss of poly(styrene sulfonic acid) leading to a decrease in conductivity. Changes in crystallinity, lamellar period, orientation and thickness of the membranes are reported and compared to corresponding properties of the initial polymer films and the pristine membranes. The membranes where most severe changes in the structure of the matrix polymer can be observed have the shortest lifetimes in the fuel cell.

1. Introduction

During the last decade the large-scale production of polymer electrolyte fuel cells (PEFC) as power sources for portable electronic devices, vehicles as well as small-scale stationary power sources has been brought into focus [1, 2]. Intensive research of the PEFC and the direct methanol fuel cell (DMFC) has lead to improvements in many crucial issues, such as reduction of the amount of catalyst. However, a remaining problem is the price of the commonly used perfluorosulfonic acid based ion exchange membranes, for example Nafion® (DuPont de Nemours & Co.). In addition, these types of material suffer from relatively high methanol crossover and therefore alternative membranes for the DMFC are needed [3]. Several different types of membranes have been developed (e.g., [4] and references therein) but none of them has so far been able to compete seriously with the commercial perfluorosulfonic acid membranes.

During this project ion exchange membranes based on commercially available poly(vinylidene fluoride) (PVDF) polymer films have been synthesized and the structure and the properties of these membranes have been studied [5–9]. The PVDF matrix has been irradiation grafted with styrene and subsequently sulfonated to attain a proton conducting PVDF-graft-poly(styrene sulfonic acid) (PVDF-g-PSSA) membrane with suitable physicochemical properties for the PEFC. As a continuation of this work, a systematic study of the influence of the fluoropolymer matrix on the structure and the properties of irradiation grafted ion exchange membranes was undertaken. Membranes based on different fluoropolymers were prepared under similar conditions [10, 11] in order to obtain membranes with comparable PSSA content and the irradiation grafting process [11], water management [12], physicochemical properties [13] and the structure [14] of the membranes have been studied.

The aim of the present study is to examine the effects of a fuel cell test on the structure of this series of irradiation grafted membranes based on seven different fluoropolymer matrices. Wide angle (WAXS) and small angle X-ray scattering (SAXS), and Raman spectroscopy were used to investigate structural changes induced by the fuel cell tests. Combining these techniques a complete picture of such changes is obtained since X-ray scattering is used to study the changes related to the crystalline phase and the ordering of the crystalline material while information about the composition, macroscopic distribution of the membrane components, and the local polymer chain conformation is obtained from Raman.

2. Experimental details

2.1. *Membranes*

The following polymers were selected as matrices: 15, 40 and 80 μm thick poly(vinylidene fluoride) films obtained from Korsnäs, Structur Oy, and Goodfellow, respectively. Two 80 μm poly(vinylidene fluoride-co-hexafluoropropylene) films (PVDF-co-HFP), containing 6 and 15% HFP, from Elf Atochem. A 50 μm poly(ethylene-alt-tetrafluoroethylene) (ETFE) film from Nowoflol and a 75 μm poly(tetrafluoroethylene-co-hexafluoropropylene) (FEP) film from DuPont. Details of the synthesis of the membranes can be found elsewhere [11]. Properties of the pristine grafted and sulfonated membranes are shown in Table 1.

2.2. *Conductivity*

The ionic conductivities of the membranes were determined from impedance spectra using data gathered in the frequency range from 5 to 85 kHz [13].

2.3. *Fuel cell measurements*

The stabilities of the membranes were investigated at a constant cell voltage of 0.4 V in a 5 cm^2 fuel cell [13]. The non-pressurized cell operated at a temperature of 60 °C with pure hydrogen and oxygen. A wet membrane and gas diffusion electrodes (ELAT® with 0.35 mg Pt cm^{-2} by E-TEK) coated with Nafion® solution (0.5–0.8 mg cm^{-2}) were clamped together in the cell with a standard torque of 5.5 Nm. A hotpressing procedure was omitted since the membranes were required for analysis after these tests though this as well as using only Nafion® as a binding ionomer reduced performance due to higher internal resistances in the cell.

2.4. *WAXS studies*

Since the samples were also required for Raman spectroscopy studies, they could not be cut or folded and the X-ray scattering measurements were made from single films with Cu$K\alpha$ radiation [14]. However, a symmetrical transmission mode was utilized since the symmetrical reflection geometry could not be used due to the roughness of the surfaces of the samples. The degree of orientation of the PVDF based samples was measured by rotating the samples about their normal using an angular step of 0.2° and a measurement time of 10 s per point. The degree of orientation of the membranes was determined by the full width at half maximum, FWHM, of the orientation distributions of the PVDF reflections (110) and (002) ($2\theta = 19.8°$ and 38.8°, respectively) by fitting a gaussian function to the data. The former reflection gives information on the lateral packing mode of the crystallites while the latter describes orientation of the ordered PVDF chains since the (002) plane is perpendicular to the PVDF chains. Since Bragg peaks corresponding to the Miller indices of

Table 1. Properties of the pristine membranes: degree of grafting (DOG), ion exchange capacity (IEC), water uptake (WU) in terms of water molecules per sulfonic acid group at room temperature under 100% relative humidity, and the lifetime (t_l) in the fuel cell

Host material	Formula of the host material	DOG /%	IEC /meq g^{-1}	WU /$N(H_2O)/(SO_3^-)$	t_l /h
PVDF-a		36–39	1.83	23	130–150
PVDF-b	id	39	1.83	20	140–160
PVDF-c	id	36	1.64	22	35–40
PVDF-co-HFP (6%)	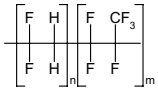	33–39	1.81	30	~150, 1 000
PVDF-co-HFP (15%)	id	35–39	1.94	39	10–20
ETFE	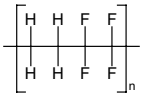	36–39	1.51	32	30–150
FEP	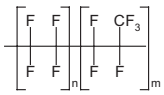	34	1.80	30	75–80

(001) could not be detected in the intensity curves of the ETFE-g-PSSA and those of polytetrafluoroethylene (PTFE) were not known, the degrees of orientation of the ETFE and the FEP based membranes were not measured.

The crystallinity of the membranes was estimated by fitting a crystalline and an amorphous model to the measured intensity curve as discussed in detail in [14]. However, here the angular range for FEP based samples was $15° < 2\theta < 50°$.

2.5. *SAXS studies*

The equipment for the SAXS measurements is described in [14]. Two different distances between the sample and the detector, 160 and 1165 mm, were used to cover magnitudes of the scattering vector, k, from 0.008 to 0.6 $Å^{-1}$ (Bragg distances from 10 to 780 Å). SAXS intensity curves of lamellar polymers show a peak arising from the lamellar structures, the position of which gives the average thicknesses of the amorphous and the lamellar layer, the lamellar period. The SAXS intensity curves of the membranes were weighted by k^2, which at small angles accounts for the Lorentz correction of the intensity curves [15]. The lamellar period, L_p, was calculated with an accuracy of $\pm 5\%$ on the basis of the position, K, of the lamellar peak as $L_p = 2\pi/K$. The K values were determined by fitting a gaussian function to the lamellar peak. SAXS intensities were measured using two different sample orientations: first the sample was placed so that the strongest intensity maximum arose from the lamellar structure and then the sample was rotated 90° from this first position.

2.6. *Raman spectroscopy*

The Raman apparatus is described in detail elsewhere [9]. The spectral resolution was better than 3 cm^{-1}. A 100y water immersion objective (NA1) to measure samples fully hydrated and a confocal hole of 200 μm were used. The resulting depth resolution for real samples is estimated to better than 8 μm by following the intensity of the PSSA mode at 1127 cm^{-1} when moving the microscope focus stepwise through the surface of a PVDF-g-PSSA membrane. When using a water immersion objective the refractive index difference between surroundings ($n_{water} = 1.33$) and the samples ($n_{fluoropolymer} \sim 1.4$) is small and hence the effect of the refractive index on the optical path was neglected. The errors of the intensity ratios that determine the degree of sulfonation and PSSA content depend on a number of parameters such as the quality of the Raman spectra, the fitted model and sample properties and can be roughly estimated as $\pm 10\%$. It should be noted that to determine the PSSA content a matrix mode is used as a reference, so the orientation of the matrix polymer plays a significant role for the value of the intensity ratio. However, a consistent orientation was used for each membrane so the values are internally comparable.

3. Results

3.1. *Structure of the matrix materials and the pristine membranes*

The WAXS intensity curves of the matrix polymer films and the pristine membranes based on PVDF-a and PVDF-co-HFP (15%) and the strongest calculated diffraction lines [16] are shown in Figure 1 and those for ETFE and FEP materials in Figure 2 (further details in [14]). The diffraction patterns of the investigated materials are typical for semicrystalline polymers and consist of clearly distinguishable reflections and an amorphous background. For the PVDF and the PVDF-co-HFP based materials the positions of the reflections are in accord with crystal form II (α-form) of PVDF [17]. At ambient temperature the crystal structure of ETFE is orthorhombic [18] while that of FEP is pseudohexagonal [19].

The crystallinity, degree of orientation, and lamellar period of the matrix polymers and the pristine grafted films are included in Table 2. These data show inherent variation in the crystallinity of the initial films and a drastic decrease in the crystallinity when the materials are grafted and sulfonated since the grafts are mainly attached in the amorphous phase of the matrix polymer [5, 11, 14] leading to expansion of the amorphous regions. The FWHMs of orientation distributions of the grafted and sulfonated PVDF and the PVDF-co-HFP based membranes increase compared to those of the initial polymer films indicating that the degree of orientation of the matrix polymer has decreased as a consequence of grafting and sulfonation in general.

The Lorentz corrected SAXS intensity curves of the PVDF-a, the PVDF-c, and the FEP based samples are shown in Figure 3 and the lamellar periods in Table 2. For the PVDF and PVDF-co-HFP based membranes the lamellae have the same orientation as the PVDF chains [20]. After grafting and sulfonation the lamellar period increases in all the membranes where it could be determined, verifying the expansion of the amorphous phase. The intensity curve of the grafted and sulfonated FEP membrane shows only an upturn towards $k = 0$ in the covered k-range and thus the lamellar period is not measurable.

Figure 4 shows Raman spectra of the pristine membranes and the corresponding matrix materials. All membrane spectra are basically combinations of a pure PSSA spectrum and the spectrum of the matrix polymer. Raman spectra of the initial PVDF and PVDF-co-HFP films are characteristic of crystal form II of PVDF [21] in agreement with the WAXS results while after grafting and sulfonation all PVDF containing membranes show an increase in the intensity of a mode at 839 cm^{-1} and, if spectra can be obtained with a sufficient quality, a low intensity mode at 513 cm^{-1} [21]. Vibrational modes at these frequencies are found in crystal form I (β-form) of PVDF where the polymer chain is in a more stretched all-trans conformation compared to the TGTG'

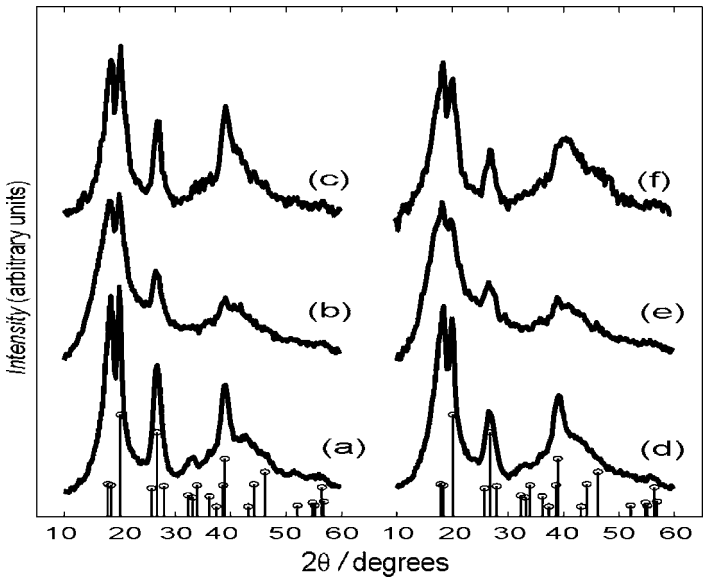

Fig. 1. WAXS intensity curves of (a) the PVDF-a matrix material, (b) the pristine grafted and sulfonated membrane PVDF-a-g-PSSA, (c) the fuel cell tested PVDF-a-g-PSSA membrane, (d) PVDF-co-HFP(15%) matrix material, (e) the pristine PVDF-co-HFP(15%)-g-PSSA and (f) the fuel cell tested grafted and sulfonated PVDF-co-HFP(15%)-g-PSSA.

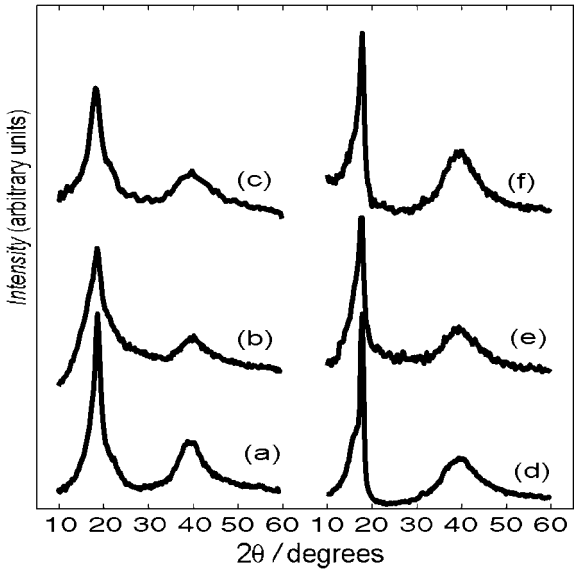

Fig. 2. WAXS intensity curves of (a) the ETFE matrix material, (b) the pristine grafted and sulfonated ETFE-g-PSSA membrane, (c) the fuel cell tested ETFE-g-PSSA, (d) the FEP matrix material, (e) the pristine grafted and sulfonated FEP-g-PSSA and (f) the fuel cell tested FEP-g-PSSA.

conformation in PVDF crystal form II [21]. Similar intensity changes are also found in spectra of uniaxially stretched PVDF films [22]. Since no change in the crystal form induced by the grafting and sulfonation is found in the X-ray data, this effect can be explained by a stretching of the polymer chain in the amorphous regions of the PVDF and PVDF-co-HFP based membranes and in the crystalamorphous interface when the membranes expand due to grafting, sulfonation and swelling with water.

An analysis of Raman spectra shows that the matrix polymer does not affect the overall efficiency of the sulfonation reaction: no unsulfonated aromatic rings can be detected and the degree of sulfonation is above 80%, estimated from the intensity ratio $I(1127)/I(1600)$ in comparison with reference samples of a known degree of sulfonation [25]. The mode at 1127 cm^{-1} is attributable to phenyl rings with a strong participation of the substituent SO_3^- [23] and the mode at 1600 cm^{-1} quantifies the total number of phenyl rings [24] (Figure 4). The ratio $I(1127)/I(1600)$ is proportional to the degree of sulfonation calculated from the ion exchange capacity, provided the sulfonic acid groups are accessible to ion exchange [25].

With the confocal Raman technique the PSSA concentration can be mapped through the membrane cross-section and in this way the local concentration and the distribution of PSSA groups can be investigated. Figure 5 shows this ratio, which is proportional to the relative concentration of PSSA, across the membrane cross-section. The ratio $I(\text{PSSA})/I(\text{matrix})$ is calculated using the integrated area of the PSSA mode at 1127 cm^{-1} (Figure 4) as a measure of the PSSA content normalized with the integrated area of an appropriate matrix mode (marked with asterisks), which was in the case of the PVDF and the PVDF-co-HFP based membranes the mode at 610 cm^{-1}, for the ETFE-g-PSSA the mode at 600 cm^{-1}, and for the FEP-g-PSSA the mode at 730 cm^{-1} [21]. The intensity ratio depends on the choice of reference mode and, in the case of the PVDF and the PVDF-co-HFP, on orientation of the sample. However, the average ratio is proportional to the degree of grafting since the fraction of nonsulfonated phenyl rings is small, as discussed above. The matrix polymer does affect the distribution of PSSA in the membrane. The PSSA concentration varies significantly across the membrane depth but is nowhere lower than a level corresponding to a degree of grafting of 20% for

Table 2. Main characteristics of the initial fluoropolymer matrix material (not grafted or sulfonated), the pristine grafted and sulfonated membranes and the fuel cell tested membranes: the structural parameters obtained from the WAXS and the SAXS results and ionic conductivities (σ) (for the tested membranes measured at the active area, see text)

Sample	Crystallinity /%	R for the determination of crystallinity	Degree of orientation (110) ($\pm 2°$)	Degree of orientation (002) ($\pm 2°$)	Lamellar period /Å (± 5 Å)	σ /mS cm^{-1}	l /μm
PVDF-a							
matrix	51	5.0	43	37	115	–	80
pristine	29	4.0	65	56	175	50	120
tested	38	6.7	46	34	90	10^{-3}	~70
PVDF-b							
matrix	57	5.2	76	66	110	–	40
pristine	23	5.0	78	73	170	50	70
tested	40	8.2	87	69	95	10^{-4}	~30
PVDF-c							
matrix	41	5.8	48	56	120	–	15
pristine	34	5.7	72	62	180	15	30
tested	43	10.3	75	–	50	10^{-3}	~10
PVDF-co-HFP (6%)							
matrix	43	3.6	46	46	115	–	80
pristine	24	3.6	63	64	190	65	120
tested	35	6.2	60	46	95	10^{-3}	65
tested II (1000 h)	43	4.2	80	57	75	10^{-1}	65
PVDF-co-HFP (15%)							
matrix	40	5.4	52	45	115	–	80
pristine	28	5.4	60	58	250	110	120
tested	36	6.3	70	67	90	10^{-4}	50
ETFE							
matrix	36	5.4	–	–	210	–	50
pristine	14	3.3	–	–	400	45	75
tested	23	7.2	–	–	–	–	40
FEP							
matrix	26	6.3	–	–	250	–	75
pristine	14	5.2	–	–	–	110	135
tested	16	5.1	–	–	–	10^{-3}	~20

The accuracy of the crystallinity determination is ±5% for the PVDF and the PVDF-co-HFP based membranes ±8% for the ETFE and FEP based membranes.

The reliability index (R) for the determination of crystallinity is the standard deviation of the fitted intensity curve from the measured one [16].

Thicknesses (l) of the membranes are determined from Raman depth scans.

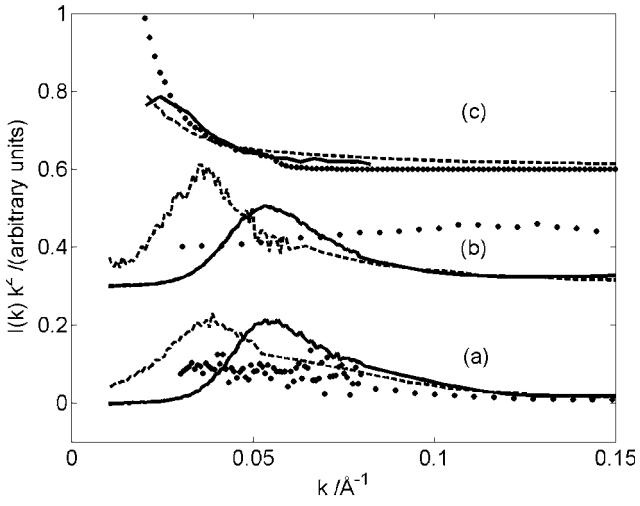

Fig. 3. SAXS intensity curves of (a) the PVDF-a, (b) the PVDF-c and (c) the FEP matrix materials as well as the corresponding pristine and fuel cell tested samples: matrix materials (——), pristine membranes (·····), and fuel cell tested samples (- - - -).

the PVDF, the PVDF-co-HFP, and the FEP based membranes. However, the ETFE-g-PSSA exhibits a significantly lower PSSA concentration at the membrane surface than the other materials, corresponding to a degree of grafting of 15% (Figure 5).

3.2. *Fuel cell tests and ionic conductivity*

Lifetimes of these experimental membranes depend on the fuel cell test conditions and under conditions used here the degradation of the membranes is accelerated. The behaviour of the membrane in the fuel cell is discussed elsewhere [13]. In short all the membranes bar the ETFE-g-PSSA are mechanically unstable. The other irradiation grafted membranes experience a rapid drop in current density during the constant voltage test (lifetimes in Table 1), while the current density for the ETFE-g-PSSA decreased steadily over a time period of 30–150 h. To determine the repeatability of the constant voltage tests trials were made and usually the difference

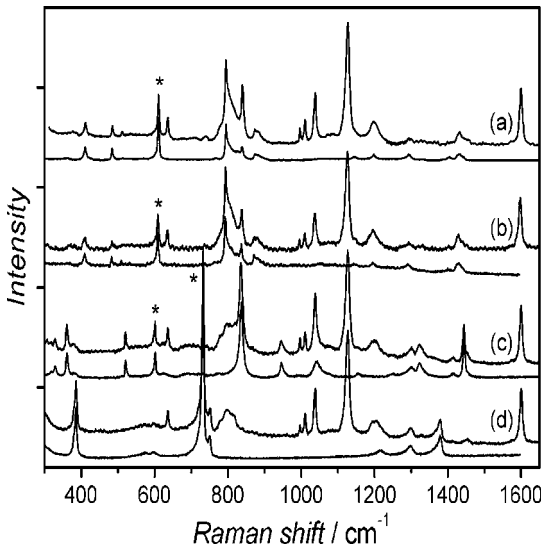

Fig. 4. Raman spectra of pristine membranes and the corresponding matrix polymers shown in pairs (pristine membrane top, matrix bottom) of (a) PVDF-a, (b) PVDF-co-HFP(15%), (c) ETFE and (d) FEP based membranes in the frequency region 350–1750 cm^{-1}. Spectra are scaled with the PSSA mode at 1127 cm^{-1} and matrix modes (see text) are marked with *. Since all PVDF and both PVDF-co-HFP based materials have similar spectra only spectra of PVDF-a and PVDF-co-HFP(15%) are included in the graph.

in the lifetime of the membranes was of the order of 10 h (Table 1). However, one of the PVDF-co-HFP (6%)-g-PSSA samples exhibited a widely different lifetime, 1000 h. To reveal reasons for this exceptional behaviour that membrane is included in this study (called PVDF-co-HFP (6%)-g-PSSA II). After the fuel cell testing the conductivity of the electrode covered area of the membranes decreased to less than 1 mS cm^{-1} (Table 2) for all the samples excluding the ETFE-g-PSSA, which was nonconductive. The conductivity of the inactive area, which is the part of the membrane covered by gaskets in the fuel cell, also decreased considerably.

3.3. *Effects of the fuel cell test on the structure of the irradiation grafted membranes*

WAXS intensity curves (Figure 1) show that the crystal structures of the fuel cell tested PVDF and the PVDF-co-HFP based membranes are still crystal form II of PVDF. Likewise the crystal structures of the ETFE and the FEP based membranes are the same (Figure 1) though both of the materials have phase transitions around the temperature region of the fuel cell tests [18, 19]: ETFE has a reversible transition centred around 60 °C while FEP has a phase transition at ambient temperatures [19]. Therefore it is expected that the ETFE and the FEP based membranes should undergo reversible phase transitions during the fuel cell test. The degree of crystallinity in the fuel cell tested membranes is higher than in the corresponding pristine membranes (Table 2) and that of the tested PVDF-c, PVDF-co-HFP (6%) II, and the PVDF-co-HFP (15%) based membranes increased to almost equal those of the corresponding matrix materials.

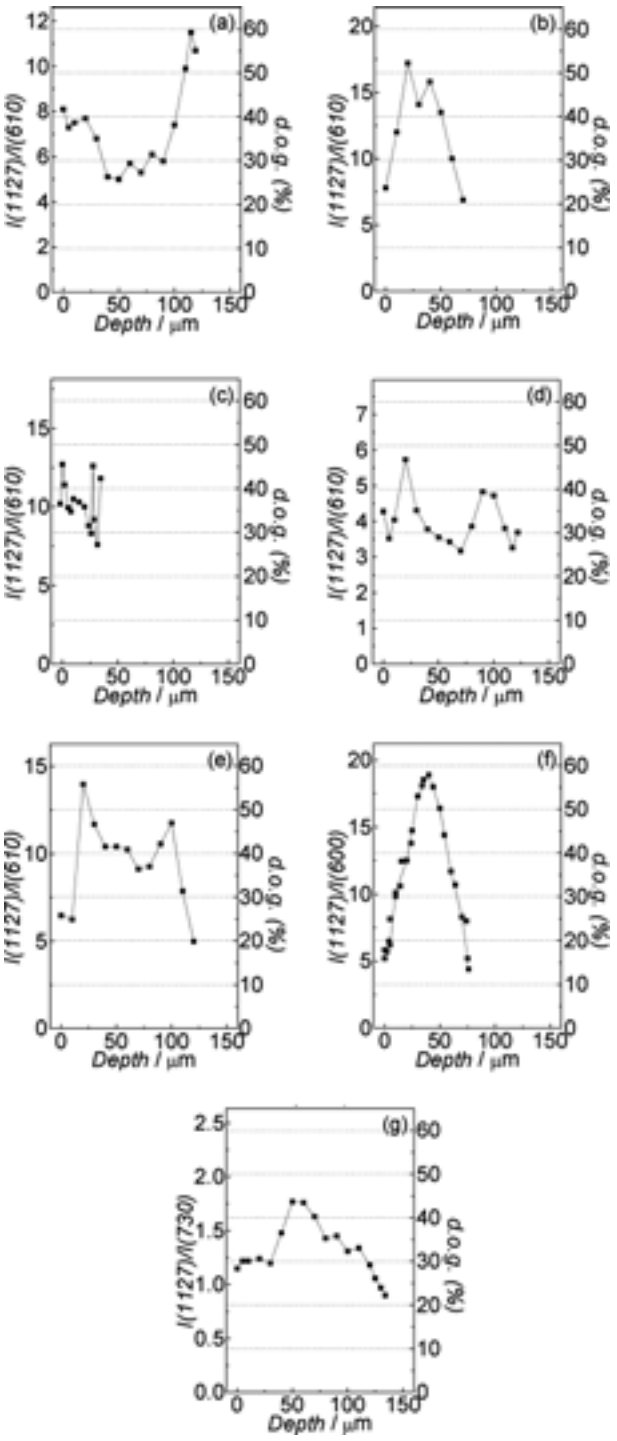

Fig. 5. Distribution of PSSA across the membrane cross-section of the pristine membranes (a) PVDF-a, (b) PVDF-b, (c) PVDF-c, (d) PVDF-co-HFP(6%), (e) PVDF-co-HFP(15%), (f) ETFE and (g) FEP based membranes as determined by Raman. PSSA concentration is given by the ratio of the intensities $I(1127)/I$(matrix reference). Right axis shows the scale normalized with the total degree of grafting.

WAXS intensity curves of the fuel cell tested PVDF and the PVDF-co-HFP based membranes (Figure 1) are more similar to the diffraction patterns of the matrix materials than those of the pristine samples. In contrast the intensity curves of the tested ETFE and the FEP based membranes are similar to the pristine samples. For the tested PVDF and the PVDF-co-HFP based mem-

branes in particular the intensity of the reflection (002) increased in the diffraction patterns. It was broad and shifted to higher angles in the intensity curve of the fuel cell tested PVDF-c, PVDF-co-HFP (6%) II, and PVDF-co-HFP (15%) based membranes. The broadening is due to a reduction in the size of the crystallites and the shift indicates that the unit cell has been slightly deformed. An orientation measurement of PVDF-co-HFP(15%)-g-PSSA confirmed that this maximum is really the reflection (002). For the PVDF-co-HFP(15%)-g-PSSA the FWHM values of the (002) orientation distribution increase during the fuel cell test (Table 2) indicating a decrease of order of crystallites. The polymer chain orientation increased for the other PVDF and the PVDF-co-HFP based membranes. The degree of orientation of the tested PVDF-co-HFP(6%)-g-PSSA II was weaker than that of the corresponding membrane with the shorter lifetime.

Figure 3 shows the SAXS intensity curves of the fuel cell tested PVDF-a, the PVDF-c, and the FEP based membranes. The pattern of the PVDF-co-HFP(15%)-g-PSSA includes a clearly distinguishable orientation dependent intensity maximum, the lamellar peak, which is also seen for the other PVDF and the PVDF-co-HFP based membranes. In the case of the fuel cell tested PVDF-c-g-PSSA membrane the difference between two SAXS intensity curves (0° and 90°) is very small indicating that the degree of orientation of the lamellae has decreased but an orientation effect still exists indicating that the structure of this membrane is still lamellar.

The lamellar peak shifts to higher angles (higher k-values) in the intensity curves of the fuel cell tested PVDF and the PVDF-co-HFP based membranes, which indicates that the lamellar period of the membrane decreased during the test (Table 2). This change was particularly noticeable for the PVDF-c-g-PSSA, which also had very low degree of orientation. The lamellae may be weakly ordered, which decreases the lamellar period. The SAXS patterns of the fuel cell tested ETFE and the FEP based membranes (Figure 3) show no intensity maximum and thus the lamellar periods of these membranes could not be determined.

The WAXS results show that the crystallinity of the fuel cell tested PVDF-a and the PVDF-b based membranes was lower (Table 2) and the degree of orientation of the crystallites of tested PVDF-a-g-PSSA was almost the same as that of the matrix materials. These results indicate that the lamellae of the fuel cell tested PVDF-a and PVDF-b based membranes are not as crystalline as the lamellae of the hosts.

Fuel cell tests of this type of membrane lead to a decrease in the concentration of the hydrophilic PSSA phase [9, 25] and consistently no or very little PSSA can be detected (the mode at 1127 cm^{-1}) in the Raman spectra of the tested membranes see (Figure 6, where the spectra of the initial matrix materials are included for comparison). To investigate the distribution of PSSA after the fuel cell test, concentration profiles of PSSA across the surfaces of the tested membranes were

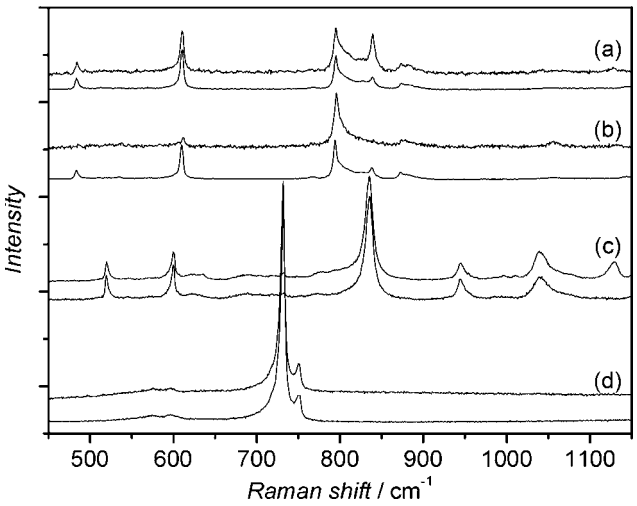

Fig. 6. Raman spectra of the fuel cell tested membranes (top) and initial polymer films (bottom) of each pair based on (a) PVDF-a, (b) PVDF-c, (c) ETFE and (d) FEP. All PVDF and PVDF-co-HFP based membranes, with the exception of PVDF-c, show the same changes in the spectra as PVDF-a and are therefore not shown in the figure.

measured. In Figure 7, the intensity ratio of the mode at 1127 cm^{-1} and the fluoropolymer reference mode, which gives a measure of the relative concentration of PSSA, is plotted for four of the membranes. The surface scans show that the residual PSSA is distributed inhomogeneously across the membrane surface. The loss of PSSA follows a similar pattern: a lower concentration of PSSA at the cathode compared to the anode surface, a low concentration in the middle of the membrane active area, and at some distance (~2 mm) outside the edge, where the membrane was clamped in the fuel cell, an increase of the PSSA concentration (at least for the PVDF-co-HFP (6%), the ETFE, and the FEP based membranes). The surface profile of the PSSA concentration of the PVDF-co-HFP(6%)-g-PSSA II is shown in Figure 7 whereas the corresponding membranes with shorter lifetime exhibited a complete loss of the PSSA even outside the active area sheltered by the gaskets.

After the fuel cell tests the all-trans chain conformation is still present in the PVDF and the PVDF-co-HFP based membranes (839 (and 513) cm^{-1} modes) showing that this conformational change is stable during the test (Figure 6). The exception is the thin PVDF-c-g-PSSA, the spectrum of which resembles that of amorphous PVDF. No changes in the matrix polymers of the tested ETFE and the FEP based membranes can be detected by Raman.

Raman spectra of a depth scan (Figure 8) from a point on the surface of the membrane facing the anode to the surface facing the cathode of the fuel cell tested PVDF-co-HFP(15%)-g-PSSA shows variations in the matrix part of the spectra at different points in the membrane cross-section. The spectra at the anode surface are similar to the PVDF-c based membrane i.e. the spectral signal of the stretched all-trans conformation of the polymer chain is not present, whilst close to

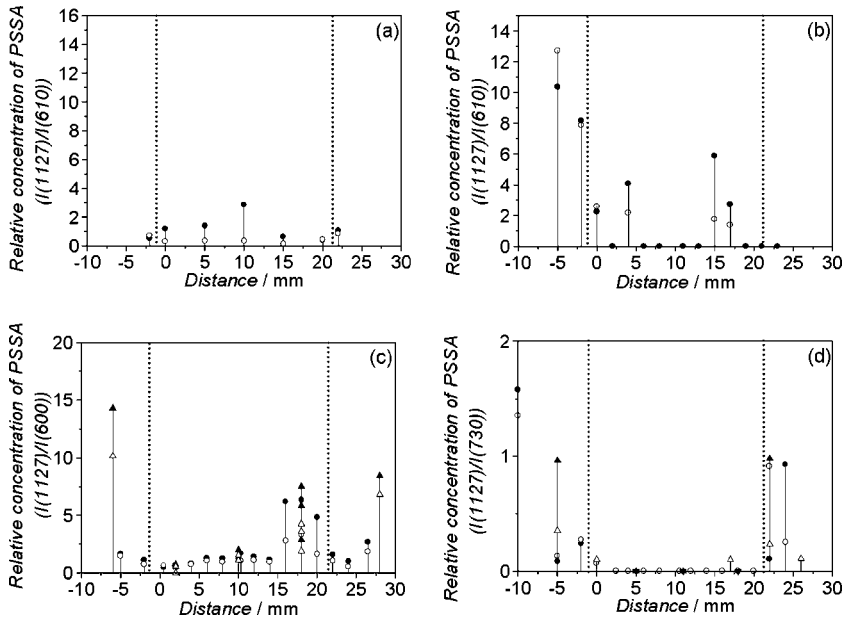

Fig. 7. Surface scans of the fuel cell tested (a) PVDF-a, (b) PVDF-co-HFP(6%) II, (c) ETFE and (d) FEP based membranes. PSSA concentration is calculated from the intensity ratio $I(1127)/I$(matrix reference). Filled symbols are points at the surface of the membrane facing the anode side, open symbols at the cathode side. Lines mark the edge of the active area where the membrane was clamped in the fuel cell.

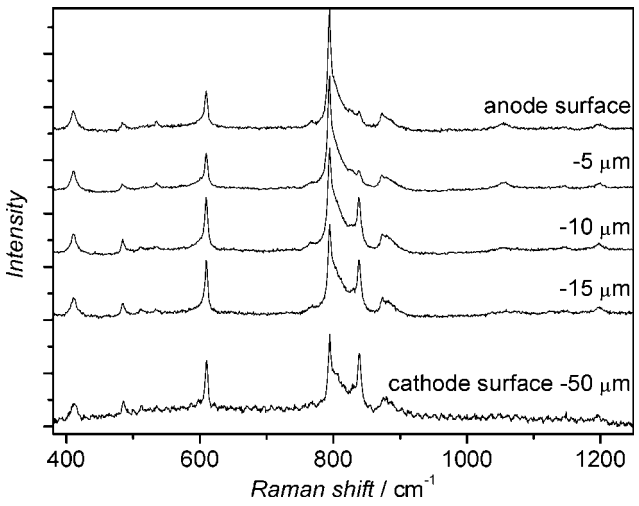

Fig. 8. Raman spectra of a fuel cell tested PVDF-co-HFP (15%) tested membrane measured from the surface of the membrane facing the anode to the surface of the membrane facing the cathode. Polymer chain conformation close to the membrane surface at the anode is changed.

the cathode the 839 cm^{-1} mode reveals that this conformation is still present. This observation suggests that the same type of significant structural change as observed for the PVDF-c based membrane takes place in the PVDF-co-HFP(15%)-g-PSSA, although on a very local scale. There seem to be points where the membrane has not been able to withstand the tensions induced during the fuel cell testing, which could explain the premature failure.

By measuring the distance from the laser focus on the top surface to the bottom surface a confocal Raman depth scan gives the membrane local thickness. Due to the loss of PSSA during the fuel cell tests (Table 2) the membranes became even thinner than the original matrix polymers. The decrease in thickness is of roughly the same magnitude for all the membranes except for the tested FEP-g-PSSA, the thickness of which was only ~25% of the initial polymer film suggesting that in addition to the structural relaxation caused by the loss of PSSA some matrix material may have been lost.

4. Discussion

Raman measurements of the pristine grafted and sulfonated membranes show that the different matrix polymers do not affect the efficiency of the sulfonation reaction significantly: the degree of sulfonation is above 80% for all the irradiation grafted membranes and no large differences in the distribution of PSSA on the membrane surface are detected. Instead the matrix material appears to affect the distribution of PSSA grafts through the membrane cross-section (Figure 5). The conductivities of pristine membranes with similar thicknesses (Table 2) have previously been connected to the water uptake of the membrane, relating a high water uptake to a high conductivity [13]. However, the conductivity of the ETFE-g-PSSA is lower than expected on the basis of its water uptake and thickness. The reason for this may be the uneven distribution of PSSA side chains with a low concentration at the surface of the membrane illustrating the necessity of a percolating network for efficient proton conduction.

After the fuel cell tests Raman spectra show a general loss of PSSA in the active area of all the membranes (Figures 6 and 7) in agreement with earlier observations [9, 26]. The degradation leads to a significant decrease in

the conductivity (Table 2) since PSSA together with water forms the proton conducting phase. However, the lifetimes in the fuel cell differ widely (Table 1) indicating variations in the chemical degradation process in the membrane based on different matrix materials.

The fuel cell tests do not change the crystal form of these semicrystalline membranes. Even the partial change in the polymer chain conformation to a more stretched all-trans conformation, observed with Raman, after the grafting and sulfonation in the PVDF and the PVDF-co-HFP based membranes remained after the fuel cell test except for the PVDF-c-g-PSSA and the PVDF-co-HFP(15%)-g-PSSA (Figure 6). The absence of the all-trans configuration found for these two membranes, which also exhibited the shortest lifetimes in the cell, suggests that large changes of the matrix structure have taken place. Thin irradiation grafted membranes have been earlier reported to suffer from mechanical failure under fuel cell conditions [27] indicating inability of the matrix material to cope with the demanding environment.

WAXS data show that the crystallinities of the fuel cell tested PVDF and the PVDF-co-HFP based samples are closer to those of the matrix materials than to the pristine membranes (Table 2), which can be attributed to a large extent to the loss of PSSA. SAXS results indicate that the decrease in the amount of PSSA, together with the reduction of the sizes of the crystallites, affects the lamellar periods of the tested PVDF and the PVDF-co-HFP based membranes, reducing the periods so that they became even shorter than in the matrix materials (Table 2). In addition, the membranes had become thinner than the initial matrix films during the fuel cell test. This suggests that there are rearrangements in the matrix structure, which may be affected by a decrease in the backbone polymer chain lengths possibly as consequence of the loss of matrix polymer material.

Raman spectra of the fuel cell tested ETFE and the FEP based membranes revealed no changes in the structure of the matrix materials in accordance with results by Brack et al. [27]. Yet on the basis of the WAXS and the SAXS measurements these materials show different behaviour than described above for the PVDF and the PVDF-co-HFP based membranes. In spite of the loss of the PSSA the degrees of crystallinity of the tested ETFE and the FEP based membranes resemble those of the pristine samples. In addition, lamellar peaks could not be measured for these fuel cell tested samples. The decrease in thickness of the ETFE-g-PSSA is similar to the other irradiation grafted membranes but the tested FEP-g-PSSA is substantially thinner than the host material. In the case of the ETFE-g-PSSA the minor change in the degree of crystallinity can be explained partly by residues of PSSA. More remarkable is the increase in the amount of amorphous material in both of these membranes at the expense of the crystalline material, which may be related to reversible phase transitions around the temperature used in the fuel cell test.

One of the fuel cell tested PVDF-co-HFP(6%)-g-PSSA membranes had clearly different lifetime of 1000 h. The corresponding membrane with the shorter lifetime lost all PSSA even outside the active area indicating that the gaskets of the cell leaked more during this test. This demonstrates the importance of applying the same conditions in the cell in order to get internally comparable results as exactly as possible.

Oxidative stability of the membranes can be studied by hydrogen peroxide test and for these membranes it has been observed that chemical degradation is accelerated by the increase in reaction surface due to a large water uptake [10]. However, in a fuel cell test the situation is not that straightforward because the changes in the hydration state of the membrane also affect the dimensions of the membrane. In addition, the loss of the hydrophilic PSSA affects the hydration and the membrane thickness. Therefore the polymer matrix experiences stress induced both by the chemical degradation and mechanical tensions and the reaction surface varies. Results obtained from the Raman spectroscopy, the WAXS and the SAXS measurements suggest that those membranes, where larger changes in the structure of the matrix material itself were detected, showed the lowest lifetimes in the fuel cell.

The lifetime of this type of irradiation grafted membrane can be increased by reducing the water uptake of the membrane along with the appropriate choice of the matrix material: the host polymer should be able to withstand the strain in the fuel cell ensuring slow chemical degradation. Therefore, too thin (PVDF-c) as well as too amorphous (PVDF-co-HFP(15%) and FEP) materials, which have high water uptake after grafting and sulfonation, should be avoided. Apparently the crystallites stabilize the structure in the membranes. If the matrix polymer itself cannot offer sufficient stability it can be made stiffer either by adding crosslinkers [27] or using sulfonation methods that allow crosslinking side reactions.

5. Conclusions

The effect of fuel cell tests on the structure of irradiation grafted membranes based on different fluoropolymer matrix materials were investigated with WAXS and SAXS methods and Raman spectroscopy. The membranes degraded chemically, losing the PSSA side chains almost completely, which resulted in a loss of conductivity.

The structure of the matrix polymers – for instance, the lamellar periods and the crystallite orientation – are affected by the fuel cell test, indicating a partial breakdown of the ordered crystalline structure. The structural rearrangements observed in the host polymer of the PVDF containing membranes were minor than in the ETFE and the FEP based membranes, both of which exhibit solid-solid phase transitions around the temperature used in the fuel cell test conceivably inducing the

changes. Among the PVDF and the PVDF-co-HFP based membranes the host material of the thinnest and the most amorphous ones suffered most evidently from the fuel cell test.

These structural changes in the matrix material are probably a consequence of a combination of the effect of chemical degradation and mechanical stress due to dimensional changes. The materials with the shortest lifetimes have a high water uptake after grafting and sulfonation, leading probably to acceleration of both of these effects. Thus, the ability of the matrix material to withstand structural changes is very important for the membrane lifetime. Materials, which are too thin or too amorphous, should be avoided, or the membrane should be made stiffer either by adding crosslinkers or using sulfonation methods that allow crosslinking side reactions.

Acknowledgements

Dr Nadia Walsby is thanked for the preparation of the membranes. The Academy of Finland (the program Electronic Materials and Microsystems), The Magnus Ehrnrooth foundation, The National Graduate School in Materials Physics (NGSMP, Finland), and MISTRA (the program Batteries and fuel cells for a better environment, Sweden) are gratefully acknowledged for financial support.

References

1. M.S. Dresselhaus and I.L. Thomas, *Nature* **414** (2001) 332.
2. B.C.H. Steele and A. Heinzel, *Nature* **414** (2001) 345.
3. C. Lamy, J.-M. Léger and S. Srinivasan, *in* J.O'M. Bockris, B.E. Conway and R.E. White (Eds), '*Modern Aspects of Electrochemistry No. 34*' (Kluwer Academic/Plenium Publishers, New York, 2001), pp. 53–118.
4. O. Savadogo, *J. New Mat. Electrochem. Systems* **1** (1998) 47.
5. S. Hietala, S. Holmberg, M. Karjalainen, J. Näsman, M. Paronen, R. Serimaa, F. Sundholm and S. Vahvaselkä, *J. Mat. Chem.* **7** (1997) 721.
6. S. Hietala, M. Paronen, S. Holmberg, J. Näsman, J. Juhanoja, M. Karjalainen, R. Serimaa, M. Toivola, T. Lehtinen, K. Parovuori, G. Sundholm, H. Ericson, B. Mattsson, L. Torell and F. Sundholm, *J. Polym. Sci., Part A: Polym. Chem.* **37** (1999) 1741.
7. T. Lehtinen, G. Sundholm, S. Holmberg, F. Sundholm, P. Björnbom and M. Bursell, *Electrochim. Acta* **43** (1998) 1881.
8. N. Walsby, M. Paronen, J. Juhanoja and F. Sundholm, *J. Polym. Sci. Part A: Polym. Chem.* **38** (2000) 1512.
9. H. Ericson, T. Kallio, T. Lehtinen, B. Mattsson, G. Sundholm, F. Sundholm and P. Jacobsson, *J. Electrochem. Soc.* **149** (2002) A206.
10. N. Walsby, '*Preparation and Characterization of Radiation-Grafted Membranes for Fuel Cells*', Doctoral thesis, University of Helsinki (2001), p. 36.
11. N. Walsby, F. Sundholm, T. Kallio and G. Sundholm, *J. Polym. Sci., Part A: Polym. Chem.* **39** (2001) 3008.
12. N. Walsby, S. Hietala, S.L. Maunu, F. Sundholm, T. Kallio and G. Sundholm, *J. Appl. Polym. Sci.* **86** (2002) 33.
13. T. Kallio, M. Lundström, G. Sundholm, N. Walsby and F. Sundholm, *J. Appl. Electrochem.* **32** (2002) 11.
14. K. Jokela, R. Serimaa, M. Torkkeli, F. Sundholm, T. Kallio and G. Sundholm, *J. Polym. Sci., Part B: Polym. Phys.* **40** (2002) 1539.
15. S. Enzo, G. Fagherazzi, A. Benedetti, and S. Polizzi, *J. Appl. Cryst.* **21** (1988) 536.
16. W. Kraus and G. Nolze, *J. Appl. Cryst.* **29** (1996) 301.
17. R. Hasegawa, Y. Takahashi, Y. Chantani and H. Tarokoro, *Polym. J.* **3** (1972) 600.
18. T. Tanigami, K. Yamaura, S. Matsuzawa, I. Masazumi, K. Mizoguchi and K. Miyasaka, *Polymer* **27** (1986) 999.
19 E. Gianetti, *Polym. Int.* **50** (2001) 10.
20. M. Torkkeli, R. Serimaa, V. Eteläniemi, M. Toivola, K. Jokela, M. Paronen and F. Sundholm, *J. Polym. Sci., Part B: Polym. Phys.* **38** (2000) 1734.
21. M. Kobayashi, K. Tashiro and H. Tadokoro, *Macromol.* **8** (1975) 158.
22. U. Hoffmann, F. Pfeifer, S. Okretic, N. Völkl, M. Zahedi and H.W. Siesler, *Appl. Spect.* **47** (1993) 1531.
23. G. Zundel, '*Hydration and Intermolecular Interaction*' (Academic Press, London, 1969), p. 116.
24. B. Jasse, R.S. Chao and J.L. Koenig, *J. Polym. Sci., Part B: Polym. Phys.* **16** (1978) 2157.
25. B. Mattsson, H. Ericson, L.M. Torell and F. Sundholm, *J. Polym. Sci., Part A: Polym. Chem.* **37** (1999) 3317.
26. F.N. Büchi, B. Gupta, O. Haas and G.G. Scherer, *Electrochim. Acta* **40** (1995) 345.
27. H.P. Brack, F.N. Büchi, J. Huslage and G.G. Scherer, Proc. 2nd International Symposium on 'Proton Conducting Membrane Fuel Cells II', S. Gottesfeld and T.F. Fuller (Eds), Vol. 98–27. The Electrochemical Society, Pennington, NJ (1999).